Available online at www.sciencedirect.com
SCIENCE DIRECT
Journal of Catalysis 238 (2006) 449–457
JOURNAL OF CATALYSIS
www.elsevier.com/locate/jcat

Development of NO sorbents tolerant to sulfur oxides

Kohei Yamamoto [a], Ryuji Kikuchi [a,*], Tatsuya Takeguchi [b], Koichi Eguchi [a]

[a] *Department of Energy and Hydrocarbon Chemistry, Graduate School of Engineering, Kyoto University, Nishikyo-ku, Kyoto 615-8510, Japan*
[b] *Catalyst Research Center, Hokkaido University, Kita 21 Nishi 10, Kita-ku, Sapporo 001-0021, Japan*

Received 27 October 2005; revised 16 December 2005; accepted 6 January 2006

Abstract

Sulfur-tolerant NO sorbents based on Pt/TiO_2 were developed by adding base oxide additives such as M_xO_y (M = Li, Na, K, Cs, Sr, Ba, La). The base oxide additives were effective in improving the NO sorption capacity of Pt/TiO_2 under both SO_2-free and SO_2-containing atmospheres. Under an SO_2-containing atmosphere, the NO sorption capacity during sorption reaction for 6 h was not affected over $Pt–Li_2O/TiO_2$ but was significantly deteriorated over the other sorbents. TPD spectra of H_2S in H_2 after a sorption reaction of 6 h in SO_2-containing atmosphere showed that SO_2 stored on $Pt–Li_2O/TiO_2$ was released at the lowest temperature. In addition to the weak basicity of lithium compared with other additives, Li_2TiO_3 formed over $Pt–Li_2O/TiO_2$ could lead to instability of the sulfates on $Pt–Li_2O/TiO_2$, giving rise to the desorption of sulfur-containing species at the lowest temperature. In situ FTIR indicated that the formation of bulk-like sulfate that needs high temperature to decompose was slow over $Pt–Li_2O/TiO_2$, which also contributed to the excellent SO_2 tolerance of $Pt–Li_2O/TiO_2$.

Keywords: NO_x storage; NO_x reduction; Sorption; Desorption; SO_2; $Pt/Li_2O/TiO_2$; Lean-burn exhaust; Diesel

1. Introduction

Diesel and lean-burn gasoline engines have better fuel economy than stoichiometric ones, and thus can lower CO_2 emissions [1–4]. In addition to automotive application, diesel engines are widely used in stationary power generation systems because of their better fuel economy. However, the exhaust gas from diesel and lean-burn engines contains several percent of O_2, which prevents conventional three-way catalysts from working effectively to reduce NO, CO, and unburned hydrocarbons [5]. Moreover, in the exhaust from diesel engines has many adverse environmental effects due to particulate matter (PM) and SO_2.

To abate NO_x under excess oxygen existing conditions, NO_x reduction techniques have been developed, including exhaust gas recirculation (EGR) [6], selective catalytic reduction (SCR) using anhydrous ammonia or aqueous urea injection [3,7–9], direct decomposition of NO over Cu/zeolite catalysts [4,10], and NO_x storage/reduction (NSR) catalysts [5,11–17]. Among these NO_x abatement technologies, NSR catalysts are expected to constitute a new NO_x control technology and represent a promising alternative to meet the upcoming regulations for NO_x emissions [13,17].

The NSR catalyst system has been commercialized for lean-burn engines in vehicle applications [11,12]. This NSR catalyst consists of precious metal and basic sorbent supported on oxides of high surface area. NO_x is first oxidized over the precious metals, then absorbed as nitrate ion in the storage component under oxidizing conditions. The stored NO_x is then reduced to N_2 on the precious metals during a short exposure to reducing atmosphere. If SO_2 originating from fuel exists in the exhaust gas, such as that from diesel engines, then SO_2 reacts with the storage component to form sulfate, which deactivates the catalyst [18–20]. Studies to date have focused mainly on $Pt–BaO/Al_2O_3$, but barium sulfate is formed in SO_2-containing exhaust, which is very stable, and consequently this catalyst requires high-temperature heating for regeneration. Therefore, sulfur poisoning will be severe and inevitable if $Pt–BaO/Al_2O_3$ is used in a sulfur-containing atmosphere, and thus NSR catalysts tolerant to sulfur poisoning are needed [19,21–23].

* Corresponding author. Fax: +81 75 383 2521.
E-mail address: rkikuchi@mbox.kudpc.kyoto-u.ac.jp (R. Kikuchi).

0021-9517/$ – see front matter
doi:10.1016/j.jcat.2006.01.006

The present study aims to develop sulfur-tolerant NSR catalysts based on TiO_2, which is known to be resistant to sulfur poisoning because sulfates on TiO_2 are less stable (due to its acidity) than those on other oxides, such as Al_2O_3 [24–26]. We focus on Pt/TiO_2, which is similar to TiO_2 from the standpoint of sulfur tolerance [27]. However, Pt/TiO_2 is expected to have little NO-sorption capacity, because nitrate is as acidic as sulfate. Consequently, we added base oxides (M_xO_y, M = Li, Na, K, Cs, Sr, Ba, La) to Pt/TiO_2 and examined the effect of the additives on the NO sorption capacity and the tolerance to SO_2 poisoning.

2. Experimental

2.1. Catalyst preparation

The samples were prepared by the impregnation method. TiO_2 (JRC-TIO-4) was impregnated with an aqueous solution of $Pt(NO_2)_2(NH_3)_2$ (Tanaka Kikinzoku Kogyo K.K.) and $M_x(NO_3)_y \cdot nH_2O$ (Wako Chemicals; M = Li, Na, K, Cs, Sr, Ba, La). The amounts of Pt and M_xO_y were 1 and 10 wt%, respectively. The mixture was kept on a steam bath at 80 °C until the solution evaporated, then dried at 120 °C overnight. The dried powders were calcined at 450 °C for 6 h in H_2 atmosphere.

2.2. NO_x removal and cyclic NO sorption–desorption tests

The resultant catalyst powders were formed into tablets, which were then pulverized to 7–11 mesh. NO_x sorption capacity was measured with a fixed-bed flow reactor with a 6-mm-i.d. quartz tube. A 1-g solid sample was fixed in the quartz tube and pretreated in He at a reaction temperature (300 °C). A gaseous mixture of 800 ppm NO, 10% O_2, and the balance He was supplied at a total gas flow rate of 60 ml min^{-1}, corresponding to 1.0 g s cm^{-3}, which corresponds to $W/F = 1.0$ g s cm^{-3}. The concentrations of NO and NO_2 in the outlet gas were measured with a chemical luminescence-type NO_x meter (Shimadzu, model NOA305). The reversible NO_x sorption–desorption performance was evaluated at 300 °C in the presence of SO_2 by switching alternately to oxidizing atmosphere (800 ppm NO, 300 ppm SO_2, 10% O_2, and balance He) for 1 h and to reducing atmosphere (5% C_3H_8/He) for 0.5 h.

2.3. Characterization of catalysts

The samples were characterized by X-ray diffraction (XRD), BET surface area, temperature-programmed desorption (TPD), and Fourier transform infrared (FTIR) spectroscopy. XRD patterns were recorded using Cu-K_α radiation on a RIGAKU Rint 2500 diffractometer for phase identification in the samples. BET surface area was measured by N_2 adsorption at the liquid nitrogen temperature using a Micromeritics Gemini 2375 analyzer. TPD measurements were performed in a fixed-bed reactor as follows: Samples were exposed to oxidizing gas (800 ppm NO, 300 ppm SO_2, 10% O_2, and the balance He) at 300 °C for 6 h, then cooled to room temperature. The samples were then heated at 5 °C min^{-1} up to 1100 °C in 5% H_2/He flow at 60 ml min^{-1}. The effluent from the reactor was analyzed by a quadruple mass spectrometer (ANELVA). The IR measurements were carried out using a SHIMAZU FTIR 8200D in diffuse reflectance Fourier-transformed infrared (DRIFT) mode with a spectral resolution of 4 cm^{-1}; 200 scans were accumulated. The powder sample was mixed with KBr in a mortar at a weight ratio of 1:5 and pretreated in He at 300 °C; then the background spectrum of the sample powder was recorded in He at 300 °C. The IR spectra under NO/O_2 or SO_2/O_2 atmosphere were measured at 300 °C by feeding a gaseous mixture of 800 ppm NO, 10% O_2, and the balance He or 500 ppm SO_2, 10% O_2, and the balance He with reference to the background spectrum. The flow rate of the gas mixture was held constant at 60 ml min^{-1}.

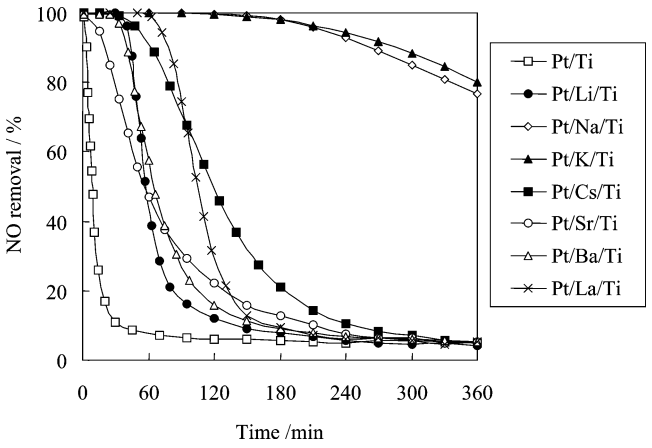

Fig. 1. NO removal by 1 wt% Pt–10 wt% M_xO_y/TiO_2 (M = Li, Na, K, Cs, Sr, Ba, La) under SO_2-free atmosphere. Reaction conditions: 800 ppm NO, 10% O_2, He balance, $T = 300$ °C, $W/F = 1.0$ g s cm^{-3}.

3. Results

3.1. NO sorption over Pt/TiO_2 modified with base oxides M_xO_y (M = Li, Na, K, Cs, Sr, Ba, La)

Fig. 1 shows NO sorption characteristics as a function of exposure time in SO_2-free atmosphere at 300 °C over Pt–M_xO_y/TiO_2 (M = Li, Na, K, Cs, Sr, Ba, La) by feeding a gaseous mixture of 800 ppm NO, 10% O_2, and the balance He at 60 ml min^{-1}. Pt/TiO_2 displayed a rapid drop in NO removal, and Pt/TiO_2 alone had quite low sorption capacity for NO. Every base oxide additive improved NO sorption capacity; among the additives, Na_2O and K_2O were especially effective in increasing NO sorption capacity, as well as in expanding the period of 100% NO removal.

Fig. 2 shows that when 300 ppm SO_2 was present in the feed gas, NO sorption capacity of the modified Pt/TiO_2 at 300 °C was significantly deteriorated, even though the sorption curve for the original Pt/TiO_2 and Pt–Li_2O/TiO_2 was identical to that without SO_2. The NO removal turned to negative values over the Cs_2O- and La_2O_3-modified Pt/TiO_2, indicating that NO sorbed on the active sites of the sorbents was released to the gas phase in the oxidative atmosphere. It may be that the nitrates sorbed on active sites of the Pt/TiO_2 modified by Cs_2O

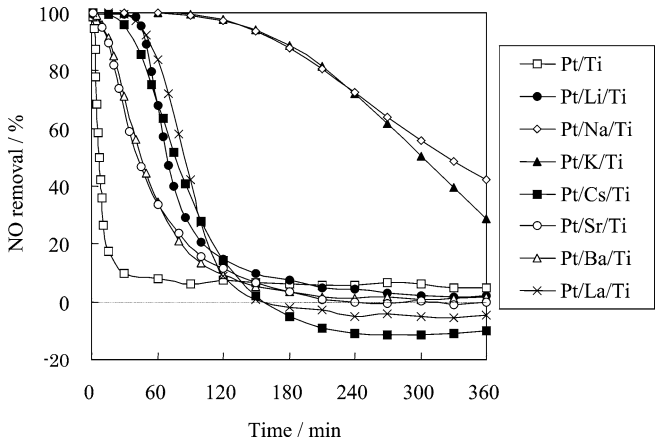

Fig. 2. NO removal by 1 wt% Pt–10 wt% M_xO_y/TiO_2 (M = Li, Na, K, Cs, Sr, Ba, La) under SO_2-containing atmosphere. Reaction conditions: 800 ppm NO, 10% O_2, 300 ppm SO_2, He balance, $T = 300\,^{\circ}C$, $W/F = 1.0\ g\,s\,cm^{-3}$.

Table 1
BET surface area, amount of NO sorption by 1 wt% Pt–10 wt% M_xO_y/TiO_2 (M = Li, Na, K, Cs, Sr, Ba, La) under SO_2-free and SO_2-containing atmosphere, and the total NO_x storage capacity calculated by assuming NO was sorbed as the nitrate over the basic additives

Sample	BET surface area ($m^2\,g^{-1}$)	Amount of NO sorption in SO_2-free atmosphere ($\times10^{-4}$ mol g^{-1})	Amount of NO sorption in SO_2-containing atmosphere ($\times10^{-4}$ mol g^{-1})	Total NO_x storage capacity calculated by assuming NO was sorbed as nitrate ($\times10^{-4}$ mol g^{-1})
Pt/TiO_2	50.7	0.60	0.60	–
$Pt–Li_2O/TiO_2$	39.5	1.70	1.72	66.9
$Pt–Na_2O/TiO_2$	28.7	6.66	5.71	32.2
$Pt–K_2O/TiO_2$	32.4	6.72	5.58	21.2
$Pt–Cs_2O/TiO_2$	50.3	2.70	1.56	7.10
$Pt–SrO/TiO_2$	47.6	1.84	1.13	9.65
$Pt–BaO/TiO_2$	52.4	1.77	1.15	6.52
$Pt–La_2O_3/TiO_2$	47.6	2.38	1.66	6.14

and La_2O_3 were replaced by SO_2 due to its stronger acidity, leading to the discharge of NO into the gas phase.

Table 1 summarizes the amount of NO sorbed under SO_2-free and SO_2-containing atmosphere as well as BET surface area of the samples, along with the total NO_x storage capacity calculated by assuming that NO was sorbed as the nitrate over the basic additives. The BET surface area of the Pt/TiO_2 modified with Cs_2O, SrO, BaO, and La_2O_3 was almost the same as that of the original, whereas greatly decreased surface area was observed for Li_2O, Na_2O, and K_2O additives. It is noteworthy that despite the decreased surface area, these additives were effective in enhancing NO sorption capacity, as shown in Fig. 1. The amount of NO sorbed was increased by adding the base oxides to Pt/TiO_2 under both SO_2-free and SO_2-containing atmospheres, and the effect of the additives on the NO sorption capacity in 6 h was in the following order: K > Na > Cs > La > Sr > Ba > Li. Because there is no clear correlation between the capacity and the BET surface area, it is likely that the NO sorption capacity depends mainly on the stability of the nitrates formed over the sorbents during the sorption reaction. The NO sorption capacity was significantly deteriorated in

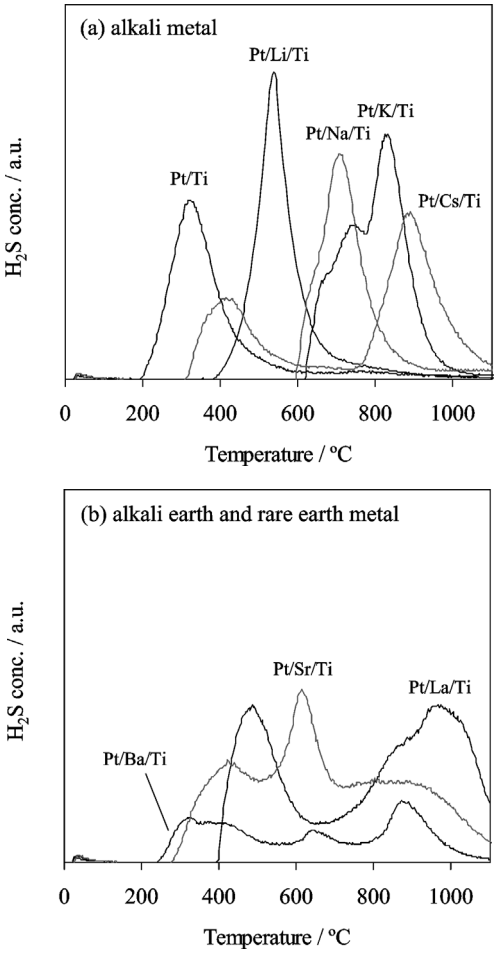

Fig. 3. TPD spectra of H_2S in 5% H_2/He after sorption reaction at 300 °C for 6 h by feeding a gaseous mixture of 800 ppm NO, 10% O_2, 300 ppm SO_2, and He balance. Heating rate, 5 °C min^{-1}; sorbents, 1 wt% Pt–10 wt% M_xO_y/TiO_2 (M = Li, Na, K, Cs, Sr, Ba, La).

SO_2-containing atmosphere for all catalysts but Pt/TiO_2 and $Pt–Li_2O/TiO_2$. Degradation in the NO sorption capacity was more evident for $Pt–Cs_2O/TiO_2$ and $Pt–La_2O_3/TiO_2$, which exhibited negative NO removal values in the later period of the sorption reaction under SO_2-containing atmosphere, as shown in Fig. 2. This may be because the sulfates formed during the sorption reaction are strongly adsorbed and stable over $Pt–Cs_2O/TiO_2$ and $Pt–La_2O_3/TiO_2$, leading to severely degraded NO sorption capacity. On the other hand, no effect of SO_2 on the NO sorption characteristics over the Li-modified Pt/TiO_2 was seen. Under SO_2-containing atmosphere, the increased sorption capacity by Li_2O was comparable to that by all of the other additives except Na_2O and K_2O, although NO sorption capacity was the least enhanced by Li_2O addition under SO_2-free conditions.

Comparing the amount of NO sorbed with the calculated total NO_x storage capacity showed that the number of Li atoms acting as NO_x sorption sites was quite small. A few percent of the added Li atoms were estimated to form $LiNO_3$, whereas 20–40% of the other basic additives were calculated to be in the nitrate form. This is partly because Li has weaker basicity compared with the other additives and partly because a new phase of weak basicity could be formed after calcination. Because of

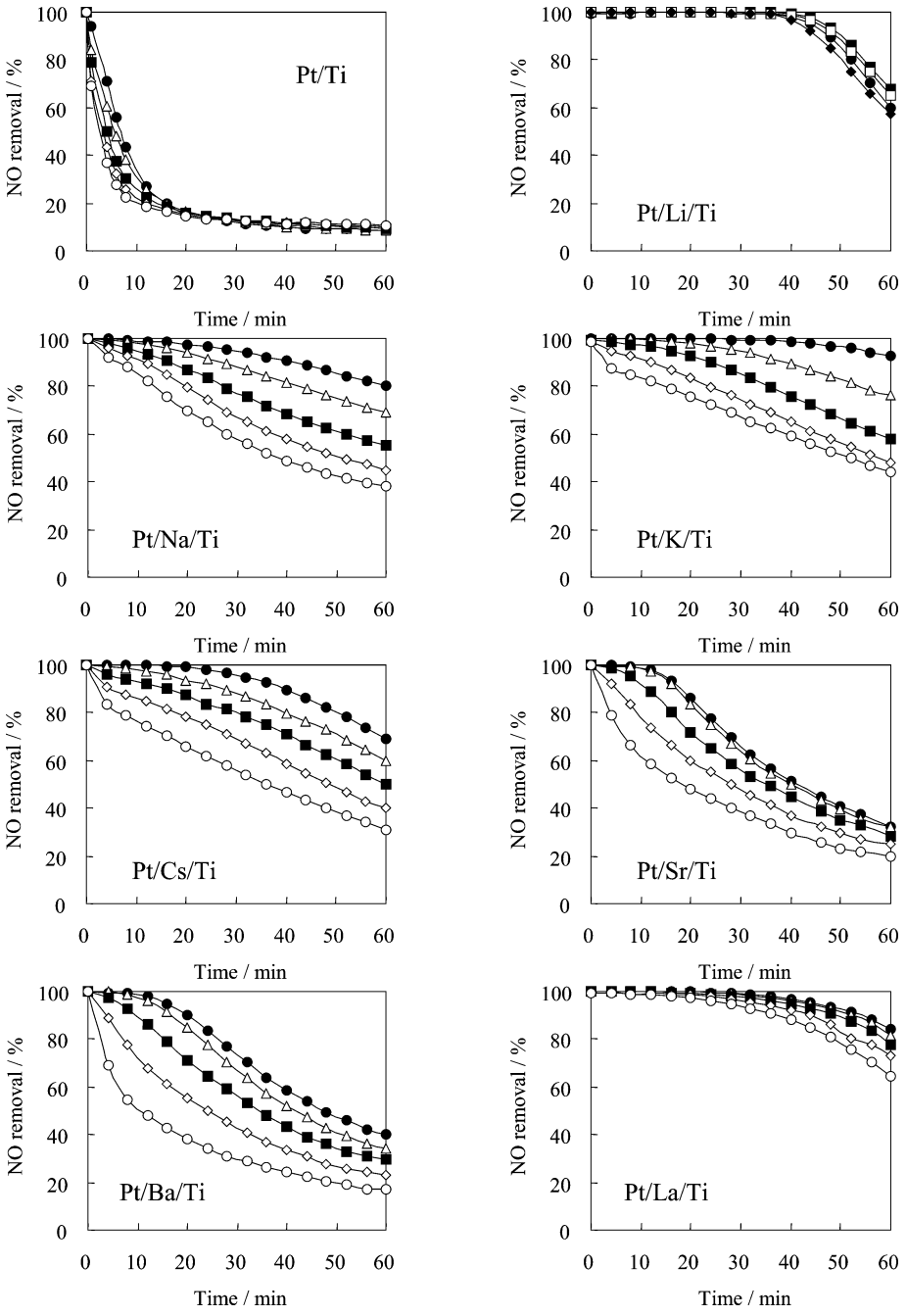

Fig. 4. NO removal by 1 wt% Pt–10 wt% M_xO_y/TiO_2 (M = Li, Na, K, Cs, Sr, Ba, La). Sorption conditions: 800 ppm NO, 10% O_2, 300 ppm SO_2, and He balance. Desorption conditions: 5% C_3H_8/He. $T = 300\,^{\circ}C$, $W/F = 1.0$ (Li, Cs, Sr, Ba, La) or 0.5 (Na, K) g s cm^{-3}. Cycle number: (●) 1st, (△) 2nd, (■) 3rd, (◇) 4th, (○) 5th, (□) 6th, and (◆) 10th.

such properties, deterioration of NO_x sorption capacity was the lowest over the Li_2O-modified Pt/TiO_2 sample.

3.2. TPD in H_2

Fig. 3 shows H_2S ($m/e = 34$) spectra desorbed in heating process under 5% H_2/He flow after exposure to oxidizing gas containing 300 ppm SO_2. No other sulfur-containing compound but H_2S was detected in the heating process, indicating that the sulfate formed under the oxidizing condition was reduced on Pt/TiO_2 to be desorbed only as H_2S. The H_2S desorption temperature was varied depending on the additives. The desorption peaks in the low-temperature range (200–500 °C) can be assigned to decomposition of the sulfate adsorbed on the TiO_2 surface, whereas those in the high-temperature range (500–1100 °C) can be assigned to a stable sulfate, such as lithium and barium sulfate formed during the SO_2 sorption reaction under the oxidizing conditions. The desorption temperature of H_2S is related to the basicity of the additives; thus, strong base additives result in formation of stable sulfates, such as cesium sulfate, which decompose at high temperatures. The amount of NO sorption on Pt–Li_2O/TiO_2 is the lowest, but the desorption

temperature of the sulfate formed is the lowest; lithium sulfate is almost completely decomposed at 600 °C.

3.3. Cyclic NO sorption–desorption over Pt–M_xO_y/TiO_2 ($M = Li, Na, K, Cs, Sr, Ba, La$)

The NO sorption–desorption performance in a cyclic operation was tested under SO_2-containing atmosphere. Fig. 4 shows NO sorption characteristics at 300 °C in the presence of SO_2 in oxidizing condition over Pt–M_xO_y/TiO_2 during cyclic sorption–desorption reactions. In these experiments, sorption reaction was carried out for 60 min in oxidizing conditions, followed by desorption reaction for 30 min in reducing conditions. Because Pt–Na_2O/TiO_2 and Pt–K_2O/TiO_2 have a large capacity for NO sorption and exhibit complete NO removal at longer than 60 min, as shown in Fig. 2, the weight of Na- and K-containing samples used in the cyclic tests was decreased to half that of the other samples, to highlight the influence of the coexisting SO_2 on NO sorption capacity over Pt–Na_2O/TiO_2 and Pt–K_2O/TiO_2. Introducing a sulfur-free gaseous mixture confirmed that the samples reversibly sorbed and desorbed NO. In the sulfur-containing atmosphere, however, the amount of NO sorbed decreased as the number of sorption–desorption cycles increased. Moreover, even in the first NO sorption process under the sulfur-containing atmosphere, NO removal was less than that under the sulfur-free conditions. These results indicate that sulfate was formed under the sulfur-containing atmosphere by oxidizing SO_2 over platinum and that the sulfate thus produced occupied the sites active for NO sorption. Nevertheless, NO removal in a cyclic manner over Pt–Li_2O/TiO_2 and Pt–La_2O_3/TiO_2 was less sensitive to coexisting SO_2 and slightly decreased in the 5th and 10th cycles for Pt–La_2O_3/TiO_2 and Pt–Li_2O/TiO_2, respectively. It is noteworthy that the amount of NO sorption on Pt–Li_2O/TiO_2 declined only slightly in the 10th cycle and that the amount of NO sorption in sulfur-containing condition is nearly equal to that in the sulfur-free atmosphere.

3.4. Effect of sorption temperature on NO removal characteristics over Pt–Li_2O/TiO_2

To analyze the sorption stability over the Li_2O-modified sample, NO sorption characteristics were investigated by changing temperature of NO sorption reaction under SO_2-free and SO_2-containing atmosphere. Fig. 5 shows temperature-programmed sorption–desorption curve of NO_x over the Pt–Li_2O/TiO_2 at a heating rate of 5 K min^{-1} and W/F of 1.0 g s cm^{-3} by feeding a SO_2-free gaseous mixture of 800 ppm NO, 10% O_2, and He balance. Complete sorption of NO was attained at the temperatures of 100–300 °C, and subsequently NO_x concentration began to increase at around 300 °C. Then NO_x concentration exceeded the initial NO level of 800 ppm in the feed at 370 °C, showed a maximum at 420 °C, and finally approached the inlet NO concentration at 500 °C. This result indicates that desorption of NO sorbed at low temperatures is dominant above 370 °C, and that NO can be effectively removed at 300 °C. Fig. 6 shows the effect of sorption reaction temperature on NO sorption characteristics under SO_2-containing atmosphere. The complete NO removal period was the longest at 300 °C and the next longest at 200 °C. A rapid drop in NO removal appeared in the very beginning of the sorption reaction at 400 °C. As for the NO sorption capacity, the amount of NO sorbed was comparable at 200 and 300 °C, whereas the sorption capacity was largely decreased at 400 °C. This is consistent with the temperature-programmed sorption of NO under SO_2-free conditions shown in Fig. 5. Thus, it is concluded that an optimum temperature for NO removal over

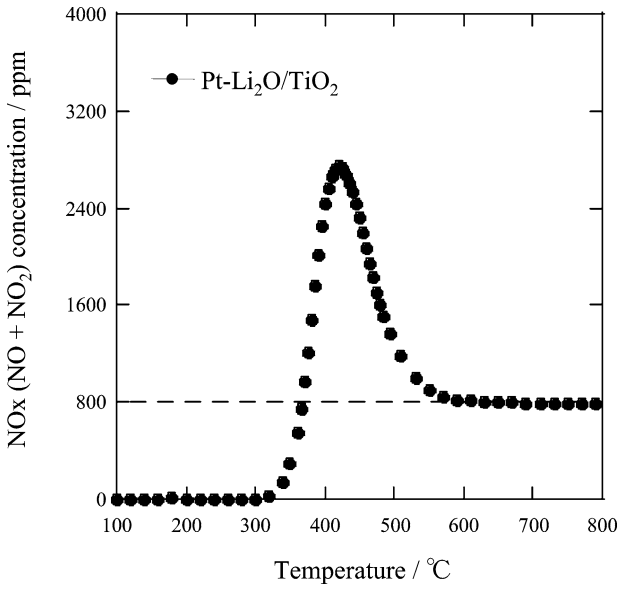

Fig. 5. Temperature-programmed sorption–desorption curve of NO_x over 1 wt% Pt–10 wt% Li_2O/TiO_2 by feeding a gaseous mixture of 800 ppm NO, 10% O_2, and He balance at a heating rate of 5 K min^{-1} and W/F = 1.0 g s cm^{-3}. (- - -) denotes the NO concentration at the inlet.

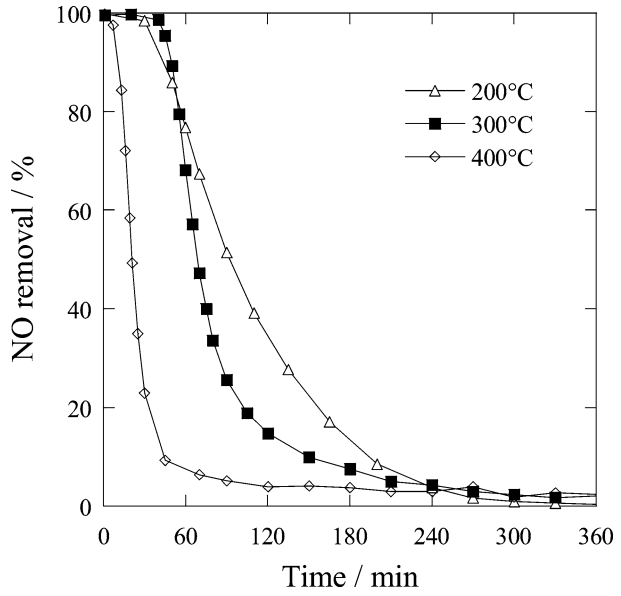

Fig. 6. Sorption curves of NO over 1 wt% Pt–10 wt% Li_2O/TiO_2 by feeding a gaseous mixture of 800 ppm NO, 10% O_2, 300 ppm SO_2, and He balance at a heating rate of 5 K min^{-1} and W/F = 1.0 g s cm^{-3}, T = 200, 300, and 400 °C.

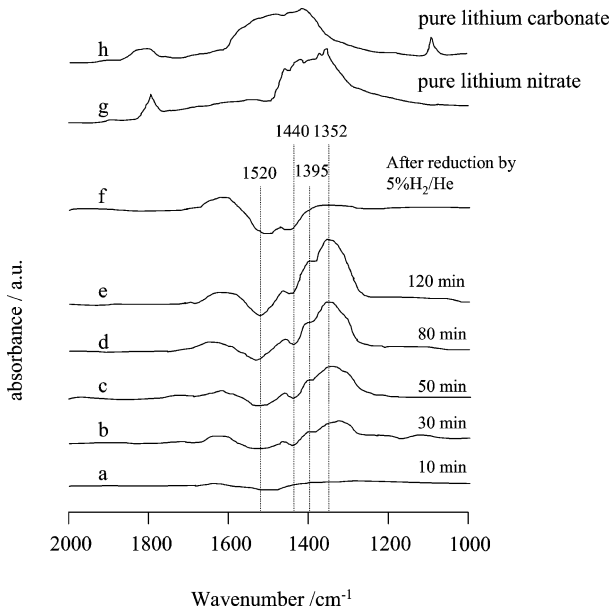

Fig. 7. IR spectra of 1 wt% Pt–10 wt% Li_2O/TiO_2 at 300 °C after exposure to 800 ppm NO and 10% O_2 in He for (a) 10, (b) 30, (c) 50, (d) 80, and (e) 120 min and (f) after reduction by 5% H_2/He. And (g) pure lithium nitrate, (h) pure lithium carbonate.

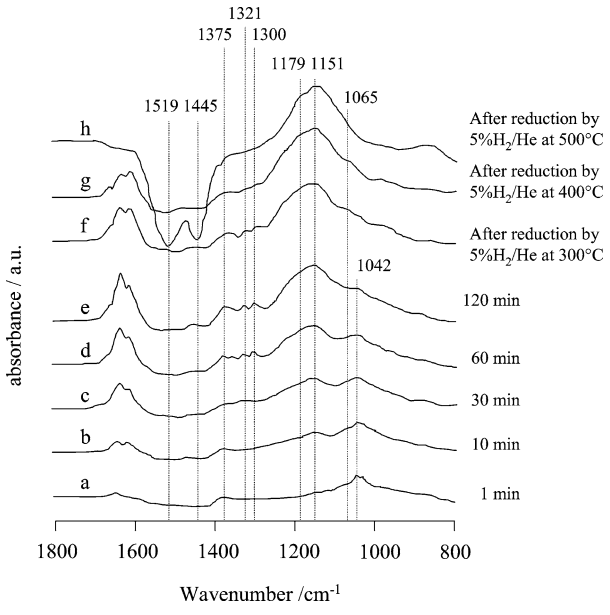

Fig. 8. IR spectra of 1 wt% Pt–10 wt% Li_2O/TiO_2 at 300 °C after exposure to 500 ppm SO_2 and 10% O_2 in He for (a) 1, (b) 10, (c) 30, (d) 60, and (e) 120 min and after reduction in 5% H_2 at (f) 300, (g) 400, and (h) 500 °C.

the Li_2O-modified sample could be 300 °C under both SO_2-free and SO_2-containing atmosphere.

3.5. *In situ FTIR*

3.5.1. *NO/O_2 sorption*

The variation of IR spectra is shown in Fig. 7 as a function of time after the exposure of Pt–Li_2O/TiO_2 to 800 ppm NO, 10% O_2 at 300 °C: (a) 10, (b) 30, (c) 50, (d) 80, and (e) 120 min after the exposure, (f) after reduction in 5% H_2/He, (g) and (h) for lithium nitrate and lithium carbonate reagents, respectively. Reference spectra in He flow were also collected at the same temperature. After 30 min of sorption, the bands in the 1300–1500 cm^{-1} range, and the negative bands at 1440 and 1520 cm^{-1} appeared. Compared with the reagent's spectra of lithium nitrate and lithium carbonate, these positive and negative spectra can be assigned to ionic nitrate and carbonate, respectively [28,29], suggesting that the carbonate formed by CO_2 in air was decomposed and replaced by nitrate during the NO sorption process. After NO sorption for 120 min, the nitrates formed during the sorption process were immediately desorbed right after switching from oxidizing atmosphere to 5% H_2, which was indicated by the disappearance of the bands in the 1300–1500 cm^{-1} range in Fig. 7f.

3.5.2. *SO_2/O_2 sorption*

Fig. 8 shows the IR spectra after exposure of Pt–Li_2O/TiO_2 to 500 ppm SO_2, 10% O_2 at 300 °C: (a) 1, (b) 10, (c) 30, (d) 60, and (e) 120 min after the exposure, and after reduction in 5% H_2/He at (f) 300, (g) 400, and (h) 500 °C. Over Pt–Li_2O/TiO_2 shown in Fig. 6, the band at 1042 cm^{-1} was observed at the beginning of SO_2/O_2 sorption, and new bands at 1065 and 1151 cm^{-1} appeared in 10 min after the sorption reaction started. The band at 1151 cm^{-1} was weak at first, then became stronger than the other bands after 30 min. Additional bands at 1300, 1321, and 1375 cm^{-1} also became stronger with increased exposure time. The bands in the 1000–1200 cm^{-1} and 1300–1400 cm^{-1} range are characteristic of ν(S–O) and ν(S=O), respectively [24,30]. The band at 1042 cm^{-1} was assigned to formation of adsorptive surface sulfate species bonded to the surface by three oxygen atoms [24,25,31], and the bands at 1065 and 1151 cm^{-1} were ascribed to lithium sulfate on surface and in bulk, respectively [32,33]. These results indicate that sulfate was formed on the surface at the very beginning of the SO_2/O_2 sorption, and subsequently stable sulfate was formed in bulk as sorption time elapsed.

To examine the stability of the sulfates over the Pt–Li_2O/TiO_2, the atmosphere was switched from SO_2/O_2 mixture to 5% H_2/He and temperature was raised stepwise from 300 °C up to 500 °C, as shown in Fig. 8, spectra (f), (g), and (h). At 500 °C, the bands of 1042 and 1065 cm^{-1} disappeared and the broad band at 1151 cm^{-1} remained. This result indicates that bulk-like sulfate existed stably even at 500 °C in the reducing atmosphere, which is consistent with the TPD results in Fig. 3, and that once the sulfate species are formed in bulk, they are more difficult to decompose compared with the surface sulfate. The negative bands assigned to carbonate were observed at 1445 and 1519 cm^{-1}, indicating carbonate was decomposed by the increase in the temperature.

The IR spectra of the other samples are shown in Fig. 9, as a function of sorption time after exposure to 500 ppm SO_2, 10% O_2 at 300 °C: (a) 1, (b) 2, (c) 5, (d) 30, and (e) 60 min. On Pt–M_xO_y/TiO_2 (M = Na, K, Cs, Sr, Ba), the bands at around 1150 cm^{-1} appeared immediately after SO_2/O_2 mixture was supplied. This band can be attributed to bulk-like sulfate, and thus it can be said that the bulk-like sulfate formation can be rapid over the modified Pt/TiO_2. In addition to this bulk-

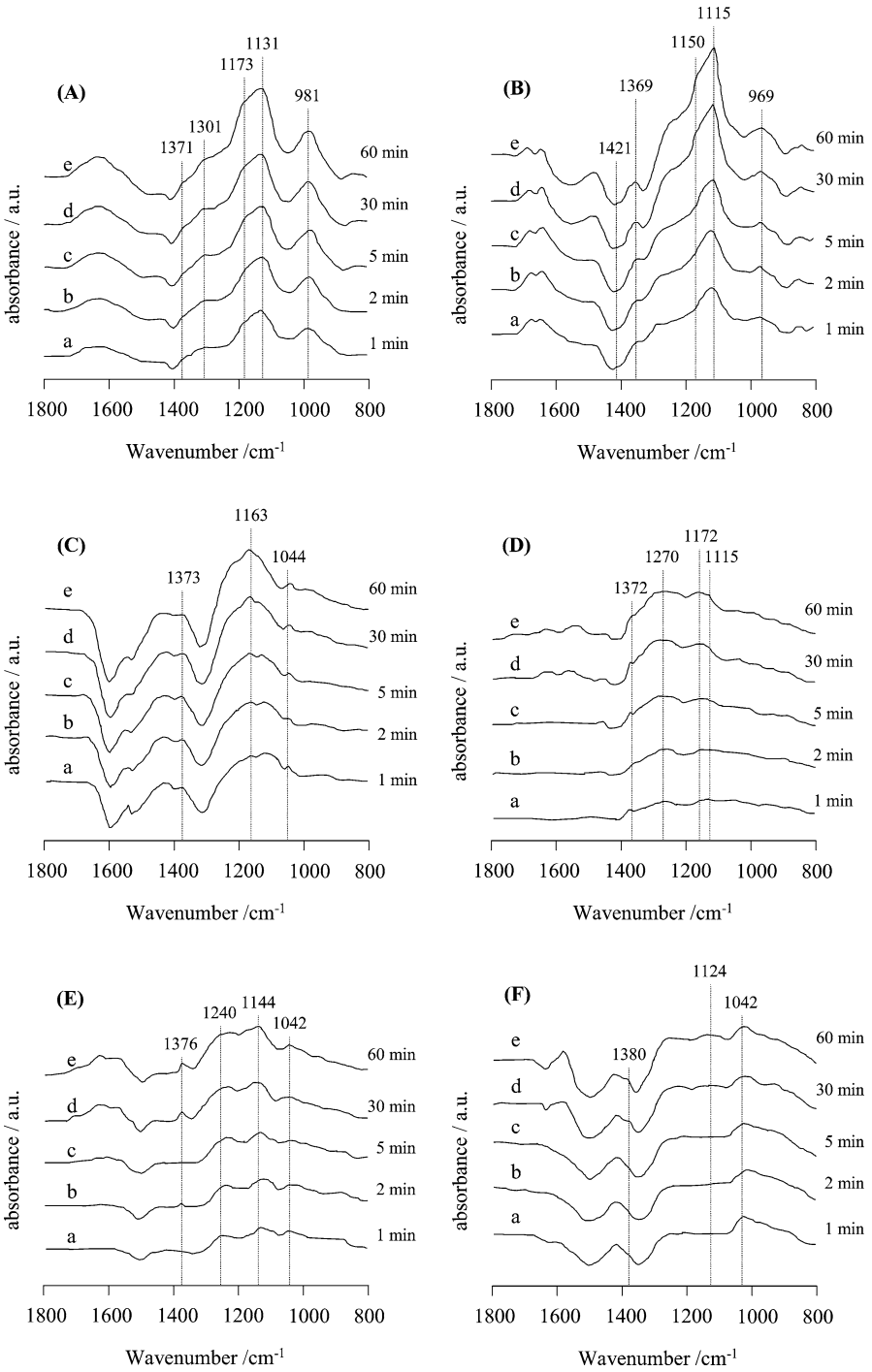

Fig. 9. IR spectra of 1 wt% Pt–10 wt% M_xO_y/TiO_2 (M = Na, K, Cs, Sr, Ba, La) at 300 °C after exposure to 500 ppm SO_2 and 10% O_2 in He for (a) 1, (b) 2, (c) 5, (d) 30, and (e) 60 min. (A) Pt/Na/Ti, (B) Pt/K/Ti, (C) Pt/Cs/Ti, (D) Pt/Sr/Ti, (E) Pt/Ba/Ti, (F) Pt/La/Ti.

like sulfate, surface sulfates can exist over Pt–K_2O/TiO_2, Pt–Cs_2O/TiO_2, Pt–SrO/TiO_2, and Pt–BaO/TiO_2, even after sorption for 120 min. This could explain the multiple peaks in the TPD profile for these samples shown in Fig. 3, because the surface sulfates tend to decompose at lower temperature than the bulk sulfates. In contrast, for Pt–La_2O_3/TiO_2, bands to the bulk sulfate are not observed after sorption for 60 min, but those to the surface sulfate are present. This is because the formation of the bulk sulfate is quite slow over Pt–La_2O_3/TiO_2. Therefore, it can be considered that because of the slow rate of the bulk sulfate formation, SO_2 is sorbed mainly as the surface sulfate in cyclic sorption–desorption operation as shown in Fig. 4, leading to better sulfur tolerance of Pt–La_2O_3/TiO_2.

4. Discussion

Lithium is a weaker base than the other components, and it exists as not Li_2O but Li_2TiO_3 in Pt–Li_2O/TiO_2 after cal-

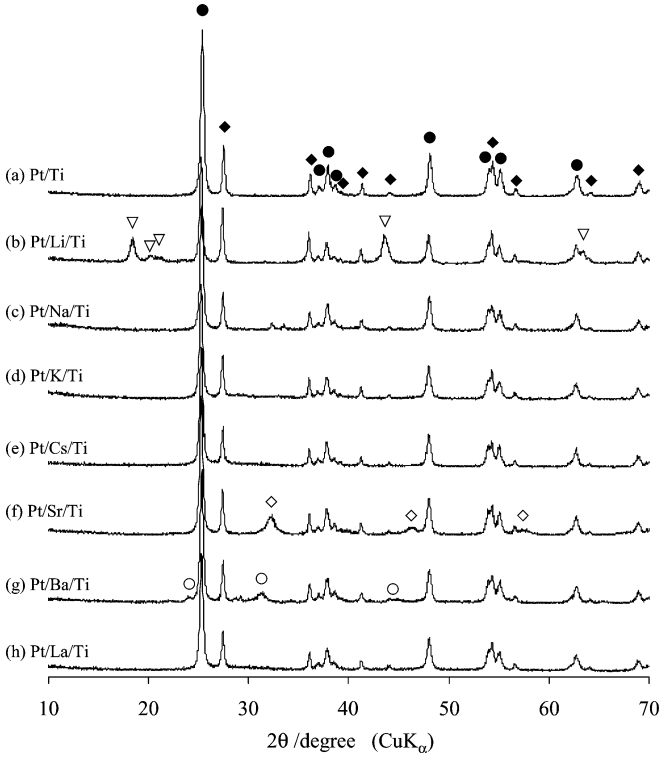

Fig. 10. XRD patterns of 1 wt% Pt–10 wt% M_xO_y/TiO_2 (M = Li, Na, K, Cs, Sr, Ba, La). (●) TiO_2 (anatase), (◆) TiO_2 (rutile), (▽) Li_2TiO_3, (◇) $SrTiO_3$, (○) $BaTiO_3$.

cination at 450 °C, as indicated by XRD in Fig. 10, and thus Pt–Li_2O/TiO_2 has even weaker basicity. As a result, though the amount of NO sorbed was less than for the other modified Pt/TiO_2, the desorption temperature of the sulfate produced during the sorption reaction was lowest, because stable sulfate formation over Pt–Li_2O/TiO_2 is difficult. Accordingly, Pt–Li_2O/TiO_2 displayed excellent tolerance to sulfur, as shown in Figs. 2 and 4. Instability of the sulfate over Pt–Li_2O/TiO_2 offers the advantage that Pt–Li_2O/TiO_2 can be easily regenerated by decomposing the sulfate by thermal treatment as high as 600 °C, even if the catalyst is partially degraded by sulfur poisoning.

In situ FTIR results of SO_2/O_2 sorption on Pt–Li_2O/TiO_2 and Pt–La_2O_3/TiO_2 revealed that SO_2 was sorbed initially as adsorptive surface sulfate species bonded to surface by three oxygen atoms and lithium or lanthanum sulfate on the surface, after which the surface sulfate was transformed into bulk sulfate. Once such sulfate species in bulk are formed, decomposing it is difficult even in reducing atmosphere, as demonstrated by TPD in Fig. 3. It is also indicated by in situ FTIR that the formation of lithium and lanthanum sulfates on Pt–Li_2O/TiO_2 and Pt–La_2O_3/TiO_2 was slower than the other catalysts. In contrast to Pt–Li_2O/TiO_2 and Pt–La_2O_3/TiO_2, over the other catalysts SO_2 was stored as stable bulk sulfate at the very beginning of exposure to SO_2/O_2 atmosphere. The slow rate of the bulk sulfate formation can be a reason for the better sulfur tolerance of Pt–Li_2O/TiO_2 and Pt–La_2O_3/TiO_2 in the alternative sorption–desorption reactions for five cycles under oxidizing SO_2-containing atmosphere, as shown in Fig. 7.

The XRD patterns in Fig. 10 show that Li_2TiO_3, $SrTiO_3$, and $BaTiO_3$ were formed over Pt–Li_2O/TiO_2, Pt–SrO/TiO_2, and Pt–BaO/TiO_2, respectively, after calcination at 450 °C. The intensity of the IR bands attributed to the sulfates formed on these samples is weaker, and thus it seems that the sulfates formed over these compounds are less stable those formed over base oxides such as SrO and BaO.

As shown in Fig. 7, NO was stored as nitrate on Pt–Li_2O/TiO_2 in the NO absorption process. The amount of NO sorbed in CO_2-containing conditions did not decrease, possibly because carbonate formed by CO_2 in air was decomposed and substituted by nitrate during the NO absorption process [28]. Consequently, NO sorption capacity should not be influenced under CO_2-containing conditions.

5. Conclusion

The effect of base oxides (M_xO_y, M = Li, Na, K, Cs, Sr, Ba, La) to Pt/TiO_2 on NO sorption capacity and tolerance to SO_2 poisoning was investigated in an effort to develop NO sorbents tolerant to sulfur oxides. Through addition of the base oxides to Pt/TiO_2, NO sorption capacity was largely improved under SO_2-free and SO_2-containing atmospheres; Pt/TiO_2 alone could sorb only a small amount of NO. Deterioration of the NO sorption capacity by SO_2 was evident over all of the modified Pt/TiO_2 catalysts except Pt–Li_2O/TiO_2. Less NO was sorbed over Pt–Li_2O/TiO_2 under SO_2-free atmosphere than over the other modified sorbents, whereas under SO_2-containing atmosphere, NO storage capacity over Pt–Li_2O/TiO_2 was unchanged and comparable to that over the other sorbents except for the Na_2O- and K_2O-modified sorbents. Lithium has weak basicity compared with the other basic additives, and Li_2TiO_3 formed on Pt–Li_2O/TiO_2 is also a weak base; thus, SO_2 was adsorbed weakly on Pt–Li_2O/TiO_2, leading to the excellent tolerance to SO_2.

Hydrogen sulfide was only the component desorbed from the modified sorbents under H_2 atmosphere. TPD of H_2S from the sorbents after sorption reaction under SO_2-containing conditions showed that H_2S was desorbed at the lowest temperature over Pt–Li_2O/TiO_2. Multiple peaks appeared at the higher-temperature range in the TPD profile for the other samples, indicating that SO_2 was sorbed stably as in various states, leading to severe SO_2 poisoning, and that high-temperature treatment was needed to decompose the sulfates. In situ FTIR revealed that bulk-like sulfates were formed immediately after exposure to SO_2/O_2 atmosphere over all sorbents except Pt–Li_2O/TiO_2 and Pt–La_2O_3/TiO_2, and that such bulk-like sulfate formation was quite slow over Pt–Li_2O/TiO_2 and Pt–La_2O_3/TiO_2.

In cyclic sorption–desorption reactions under SO_2-containing conditions, NO removal was largely degraded over all of the modified sorbents except Pt–Li_2O/TiO_2 and Pt–La_2O_3/TiO_2 as the number of cyclic operations increased. Over the degraded samples, the bulk sulfates were formed immediately in the sorption process and were not released in the desorption process due to the material's stability, leading to the severe SO_2 poisoning. In contrast, because of the slow rate of bulk sulfate formation over Pt–Li_2O/TiO_2 and Pt–La_2O_3/TiO_2, as well as the insta-

bility of the sulfate over Pt–Li_2O/TiO_2, the decrease in NO storage capacity was insignificant over Pt–Li_2O/TiO_2 and Pt–La_2O_3/TiO_2 after the cyclic sorption–desorption tests.

Acknowledgment

This work was supported by Grants-in-Aid for Scientific Research (Project No. 16360402) from the Japanese Society for the Promotion of Science (JSPS).

References

[1] J.C. Frost, G. Smedler, Catal. Today 26 (1995) 207.
[2] J.C. Clerc, Appl. Catal. B: Environ. 10 (1996) 99.
[3] R.J. Farrauto, K.E. Voss, Appl. Catal. B: Environ. 10 (1996) 29.
[4] K.M. Adams, J.V. Cavataio, R.H. Hammerle, Appl. Catal. B: Environ. 10 (1996) 157.
[5] W.S. Epling, J.E. Parks, G.C. Campbell, A. Yezerets, N.W. Currier, L.E. Campbell, Catal. Today 96 (2004) 21.
[6] M. Zheng, G.T. Reader, J.G. Hawley, Energy Convers. Manage. 45 (2004) 883.
[7] M. Shelef, Chem. Rev. 95 (1995) 209.
[8] W.E.J. van Kooten, H.P.A. Calis, C.M. van den Bleek, Stud. Surf. Sci. Catal. 116 (1997) 357.
[9] M. Koebel, M. Elsener, M. Kleemann, Catal. Today 59 (2000) 335.
[10] J.N. Armor, K. Li, Appl. Catal. B: Environ. 5 (1995) 257.
[11] S. Matsumoto, Catal. Today 29 (1996) 43.
[12] N. Miyoshi, S. Matsumoto, T. Tanizawa, T. Tanaka, S. Tateishi, K. Kasahara, Catal. Today 27 (1996) 63.
[13] S. Hodjati, P. Bernhardt, C. Petit, V. Pitchon, A. Kiennemann, Appl. Catal. B: Environ. 19 (1998) 209.
[14] S. Hodjati, K. Vaezzadeh, C. Petit, V. Pitchon, A. Kiennemann, Catal. Today 59 (2000) 323.
[15] V.G. Milt, C.A. Querini, E.E. Miro, M.A. Ulla, J. Catal. 220 (2003) 424.
[16] R.L. Muncrief, K.S. Kabin, M.P. Harold, AIChE J. 50 (2004) 2526.
[17] K.S. Kabin, R.L. Muncrief, M.P. Harold, Catal. Today 96 (2004) 79.
[18] P. Engstrom, A. Amberntsson, M. Skoglundh, E. Fridell, G. Smedler, Appl. Catal. B: Environ. 22 (1999) L241.
[19] S. Matsumoto, Y. Ikeda, H. Suzuki, M. Ogai, N. Miyoshi, Appl. Catal. B: Environ. 25 (2000) 115.
[20] Ch. Sedlmair, K. Seshan, A. Jentys, J.A. Lercher, Catal. Today 75 (2002) 413.
[21] K. Yamazaki, T. Suzuki, N. Takahashi, K. Yokota, M. Sugiura, Appl. Catal. B: Environ. 30 (2001) 459.
[22] H.Y. Huang, R.Q. Long, R.T. Yang, Appl. Catal. B: Environ. 33 (2001) 127.
[23] H. Hirata, I. Hachisuka, Y. Ikeda, S. Tsuji, S. Matsumoto, Top. Catal. 16/17 (2001) 145.
[24] M. Waqif, J. Bachelier, O. Saur, J.C. Lavalley, J. Mol. Catal. 72 (1992) 127.
[25] O. Saur, M. Bensitel, A.B.M. Saad, J.C. Lavalley, C.P. Tripp, B.A. Morrow, J. Catal. 99 (1986) 104.
[26] S. Matsuda, A. Kato, Appl. Catal. 8 (1983) 149.
[27] Y. Chen, Y. Chen, W. Li, S. Sheng, Appl. Catal. 63 (1990) 107.
[28] H. Mahzoul, J.F. Brilhac, P. Gilot, Appl. Catal. B: Environ. 20 (1999) 47.
[29] C. Sedlmair, K. Seshan, A. Jentys, J.A. Lercher, J. Catal. 214 (2003) 308.
[30] M. Waqif, P. Bazin, O. Saur, J.C. Lavalley, G. Blanhard, O. Touret, Appl. Catal. B: Environ. 11 (1997) 193.
[31] H. Mahzoul, L. Limousy, J.F. Brilhac, P. Gilot, J. Anal. Appl. Pyrolysis 56 (2000) 1179.
[32] C. Sedlmair, K. Seshan, A. Jentys, J.A. Lercher, Catal. Today 75 (2002) 413.
[33] J. Wang, C. Lie, Appl. Surf. Sci. 161 (2000) 406.